

See discussions, stats, and author profiles for this publication at: <https://www.researchgate.net/publication/6994129>

# Photochemistry via Photoelectron Spectroscopy: N-Substituted Phthalimides

ARTICLE *in* THE JOURNAL OF PHYSICAL CHEMISTRY A · JULY 2006

Impact Factor: 2.69 · DOI: 10.1021/jp057269v · Source: PubMed

---

CITATIONS

5

---

READS

5

2 AUTHORS, INCLUDING:



Igor Novak

Charles Sturt University

211 PUBLICATIONS 963 CITATIONS

SEE PROFILE

# Photochemistry via Photoelectron Spectroscopy: N-Substituted Phthalimides

Igor Novak\*

Charles Sturt University, POB 883, Orange NSW 2800, Australia

Branka Kovač

Physical Chemistry Division, "R. Bošković" Institute, HR-10002 Zagreb, Croatia

Received: December 13, 2005; In Final Form: April 28, 2006

The electronic structures of several N-substituted phthalimides have been investigated by UV photoelectron spectroscopy and outer valence Greens function calculations. Some spectra reveal the presence of photofragmentation and photoelimination processes related to the decay of the aminium radical cation. We compared the fragmentation mechanisms in the gas phase and in the solution.

## Introduction

Phthalimides are compounds that participate in numerous photochemical reactions of synthetic interest in solution. These reactions often involve photoinduced single electron transfer (SET) with the aid of photosensitizer.<sup>1</sup> During SET, the tertiary amine is first converted into a reactive intermediate: aminium radical (Scheme 1). Subsequently, the aminium radical may follow several decay pathways (e.g.,  $\alpha$ -CH deprotonation, decarboxylation, desilylation, retro-aldol fragmentation, or back-electron transfer).<sup>1d</sup>

The mechanism in Scheme 1 applies to processes in solution, and it can be expected that the decay of the aminium radical cation in vacuo proceeds via different mechanisms. Fragmentation reactions that are important in SET photochemistry lead to synthetically useful products. The knowledge of how electronic structure and substitution pattern affect fragmentation is important for designing efficient SET photochemical processes. The photochemical reactions involving phthalimide substrates are useful in the synthesis of heterocyclic compounds, macrocycles, or Grignard-like products.<sup>1a–c</sup> Since the radical cation generated via photoinduced SET (in solution) is the crucial intermediate, the understanding of its electronic structure is of considerable interest. Radical cations that are generated by SET in solution-based reactions can also be obtained without photosensitizers (e.g., by direct irradiation with vacuum ultraviolet (VUV) light in vacuo).

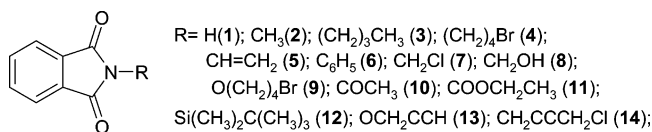
In UV photoelectron spectroscopy (UPS), VUV radiation ionizes the molecule and produces radical cations in different electronic states. Radical cations are thus generated in the gas phase directly (i.e., without electron transfer sensitizer). The UPS method is suitable for studying not only the electronic structure of radical cations, but also their possible fragmentation pathways. The products of fragmentation often include small molecules that arise due to the elimination of electrofugal functional groups from the radical cation. The fragmentation can be monitored by UPS in situ, because UPS spectra of small molecules can be readily identified. UPS spectra of small molecules have only a few well-resolved, sharp bands with characteristic ionization energies.

UPS of phthalimides **1–6** (Scheme 2) has been reported previously.<sup>2–6</sup> However, their spectra did not show evidence

## SCHEME 1



## SCHEME 2



of fragmentation processes pertaining to the aminium radical. In this work, we studied phthalimide derivatives **7–14** to obtain new information on their electronic structure and photochemistry.

## Experimental and Computational Methods

The samples of **7–14** were purchased from Acros Organics NV and Fluka AG and used without further purification (except for **10**) after checking their identity by NMR and mass spectroscopy.

The sample inlet temperatures were 100, 130, 160, 120, 110, 120, 120, and 140 °C for **7–14**, respectively. These temperatures were necessary to obtain sufficient vapor pressure in the ionization region. Due to the poor volatility of some compounds, only their HeI spectra could be measured. The HeI/HeII photoelectron spectra were recorded on the Vacuum Generators UV-G3 spectrometer and calibrated with small amounts of Xe or Ar gas, which was added to the sample flow. The spectral resolution in HeI and HeII spectra was 25 and 70 meV, respectively, when measured as fwhm of the  $3p^{-1} \ ^2P_{3/2} \text{ Ar}^+ \leftarrow \text{Ar} \ (^1S_0)$  line. The resolution in the HeII spectra was always inferior to that in HeI, which implies that some bands that are well-resolved in HeI may be unresolved in the corresponding HeII spectrum.

We have checked for the possible thermal rather than photochemical decomposition of samples. This was done by visual inspection of the sample residues in the sample inlet after UPS measurements (checking for possible color changes) and by mass spectrometry (MS) of the residue. The sample residues were obtained by cooling the walls of the sample inlet probe

Corresponding author. E-mail: inovak@csu.edu.au.

**TABLE 1: Experimental ( $E_i$ /eV) and Calculated (GF/eV) Vertical Ionization Energies of Phthalimides<sup>a,b</sup>**

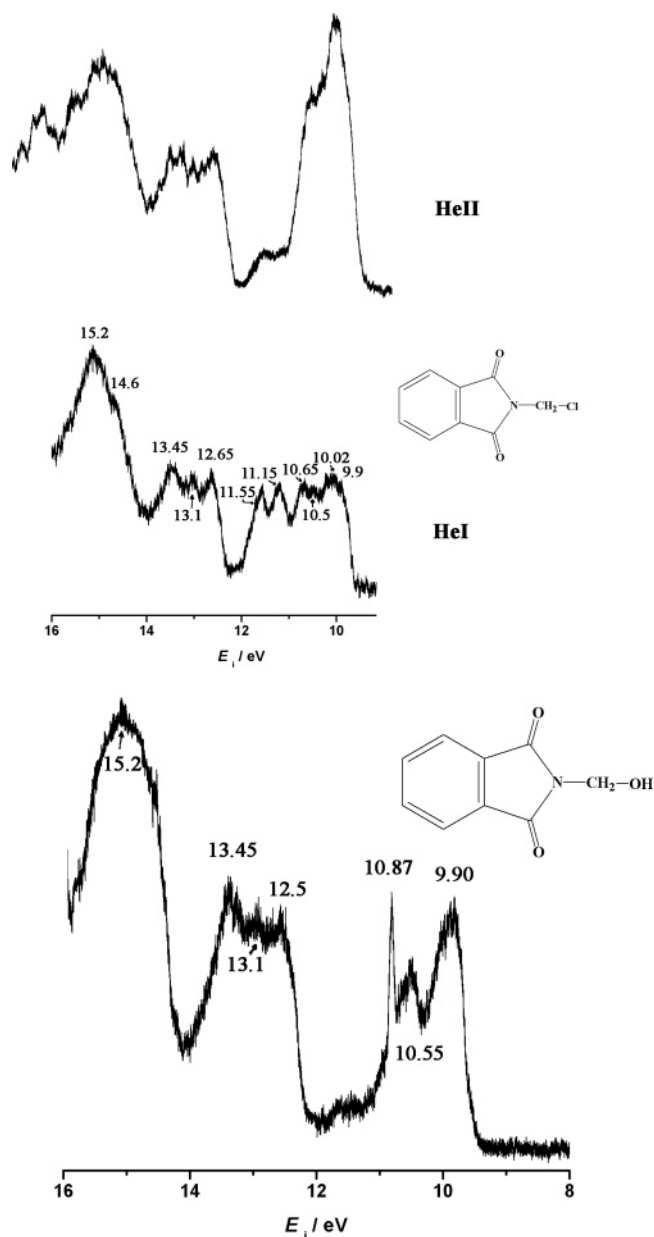
| mole-<br>cule | band | $E_i$             | OVGF                            | assignment  |
|---------------|------|-------------------|---------------------------------|---|
| 12            | X-B  | 9.78, 9.80, 10.02 | 9.43, 9.52, 10.0                | $\pi_3$ , n-, $\pi_2$                               |
|               | C-D  | 10.56, 10.68      | 10.2, 10.69                     | $n^+$ , $\pi_N$                                     |
| 23            | X-B  | 9.55, 9.9, 9.9    | 9.22, 9.43, 10.0                | $\pi_3$ , n-, $\pi_2$                               |
|               | C-D  | 10.15, 10.5       | 10.54, 11.15                    | $n^+$ , $\pi_N$                                     |
| 7             | X,A  | 9.9, 10.02        | 9.53, 9.67                      | $\pi_3$ , n-  |
|               | B-D  | 10.5, 10.65       | 10.36, 10.78, 10.94             | $\pi_2$ , $n^+$ , $\pi_N$                           |
|               | E,F  | 11.15, 11.55      | 11.0, 11.67                     | $n_{Cl}$  |
| 8*            |      | 9.90              | 9.31, 9.43                      | phthalimide   |
|               |      | 10.55             | 10.22, 10.53                    |   |
|               |      | 10.87             | 11.15, 11.21                    | HCOH  |
| 9             | X,A  | 9.25, 9.85        | 9.40, 9.60                      | $\pi_3$ , n-  |
|               | B-E  | 10.15, 10.4       | 10.06, 10.11, 10.13, 10.42      | $\pi_2$ , [ $n_{NO} - \pi_N$ ], $n_{Br}$ , $n_{Br}$ |
| 10            | F-G  | 11.1, 11.7        | 11.36, 11.68                    | $n^+$ , [ $n_{NO} + \pi_N$ ]                        |
|               |      | 9.9               | 9.58, 9.64                      | $\pi_3$ , n-  |
|               |      | 10.3, 10.55       | 10.29, 10.54                    | $\pi_2$ , $\pi_N$                                   |
| 11            | X-D  | 11.3, 11.7        | 10.87, 11.80, 12.87             | $n^+$ , $n_{CO}$ , $\sigma$                         |
|               |      | 10.0–10.3         | 9.50, 9.57, 10.45, 10.67, 10.86 | $\pi_3$ , $n_O$ , $\pi_2$ , $\pi_N$ , $n_O$         |
| 12            | E-F  | 11.25             | 11.42, 11.90                    | $n_O$ , $n_{OEt}$                                   |
|               |      | 9.2, 9.4, 9.7     | 9.19, 9.35, 9.37, 9.75          | $\pi_N$ , $\pi_3$ , n-                              |
|               |      | 10.2              | 10.40, 10.78, 10.83             | $\pi_2$ , $n^+$                                     |
| 13            | X-B  | 11.3              | 11.13, 11.40                    | s   |
|               |      | 9.55, 9.95        | 9.37, 9.56, 10.2                | $\pi_N$ , n-, $\pi_3$                               |
|               | C-D  | 10.45             | 10.33, 10.38                    | $\pi_2$ , $\pi_{CC}$                                |
| 14            | E-F  | 11.0, 11.65       | 10.46, 11.39                    | $n^+$ , $n_{OR}$                                    |
|               | X-D  | 9.6, 10.2         | 9.36, 9.53, 9.8, 9.87, 10.3     | $\pi_3$ , n-, $\pi_2$ , $\pi_N$ , $n^+$             |
|               | E-F  | 10.85             | 10.7, 10.99                     | $\pi_{CC}$  |
|               | G-H  | 11.35             | 11.06, 11.40                    | $n_{Cl}$  |

<sup>a</sup> Molecules marked with asterisk undergo photoinduced fragmentation, and the observed bands correspond to superimposed spectra of fragmentation products rather than to the parent compound; some fragmentation products are identified in the "assignment" column. GF results listed for such molecules are given in italics and refer to the parent molecule that was fragmented. <sup>b</sup> Superscripts are references from which the spectral data were taken.

(not the sample holder) with liquid nitrogen and MS examination of the crystals formed on the walls upon cooling. Also, samples were subject to several freeze–thaw cycles using the Kofler melting point apparatus. The samples were heated above the melting point (up to the UPS measurement temperature) and then cooled below melting until they crystallized. The crystals thus obtained had the same melting point as the original sample. This suggests that no pyrolysis took place during the UPS measurements and that fragmentation observed in the spectra was due to the photochemical processes. Furthermore, the measured UPS spectra were reproducible under different heating regimes.

Relative intensities of halogen lone pair ionization bands decrease significantly on going from HeI to HeII radiation. Such changes are caused by variations of atomic photoionization cross sections with electron energy and are well-established in UPS work.<sup>7</sup> The intensity variations helped us to identify bands corresponding to halogen lone pair ionizations.

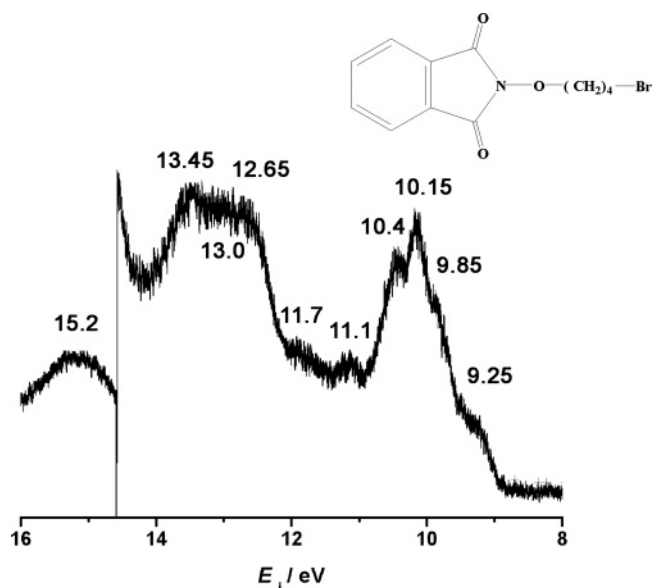
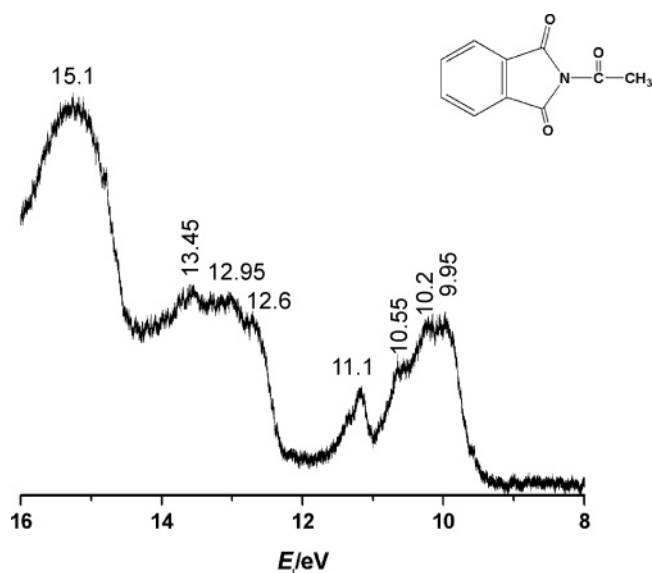
The quantum chemical calculations were performed with the Gaussian 03 program,<sup>8</sup> including full geometry optimization at the B3LYP/6-31G\* level as the first step. Subsequently, the optimized geometry was used as the input into the single-point calculation by the outer valence Greens function (OVGF) method.<sup>9</sup> The OVGF method allows direct calculation of vertical ionization energies without relying on Koopmans approximation. We performed calculations for **1** and **2**, whose spectra were assigned previously, to test the suitability of the method for spectral assignment (Table 1).



**Figure 1.** HeI and HeII photoelectron spectra of **7** and HeI photoelectron spectrum of **8**.

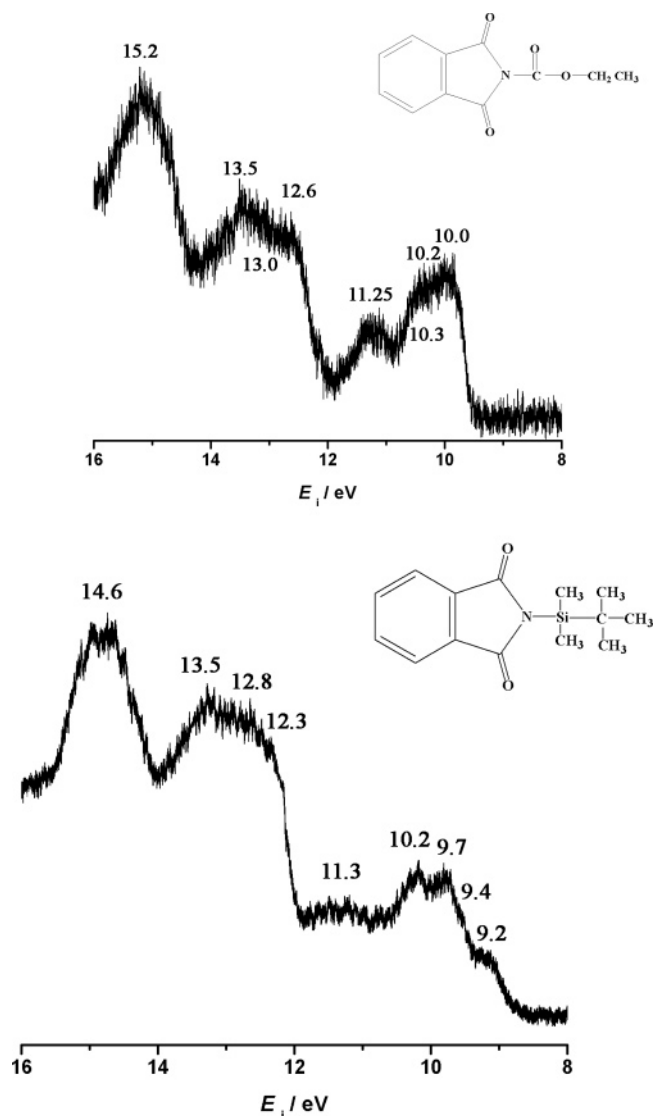
## Results and Discussion

**General Comments.** The photoelectron spectra of **7–14** are shown in Figures 1–5, and their assignments are summarized in Table 1. Due to the high density of ionic states above 12 eV, we confined our analysis to bands whose ionization energies are below that value. The interpretation of spectra was based on the comparison with previously reported spectra of N-substituted phthalimides<sup>2–6</sup> and other related molecules, HeI/HeII intensity variations, and OVGF calculations. The ratios of atomic photoionization cross sections for C2, N2p, O2p, and Cl3p orbitals are 0.31, 0.45, 0.64, and 0.05, respectively.<sup>7</sup> This information is useful for establishing the AO character of individual MO from which electrons were ejected. The bands whose relative intensities decrease least correspond to molecular orbitals with significant oxygen and nitrogen character. The halogen lone pair bands (Cl3p, Br4p) on the other hand show the most pronounced decrease in intensity on going from HeI to HeII radiation.

Figure 2. HeI photoelectron spectrum of **9**.Figure 3. HeI photoelectron spectrum of **10**.

**Assignment and Photochemistry.** The spectrum of **7** (Figure 1) shows two bands at 11.15 and 11.55 eV whose intensities decrease strongly on going from HeI to HeII radiation. These bands can be attributed to chlorine lone pair ionizations ( $n_{\text{Cl}}$ ). The bands at 9.9, 10.02, and 10.65 eV correspond to ionizations from the  $\pi$ -orbitals localized on the aromatic ring ( $\pi_3$  and  $\pi_2$ ), to the in-phase and out-of-phase linear combinations of in-plane carbonyl oxygen lone pairs ( $n_+$ ,  $n_-$ ), and to the nitrogen lone pair ( $\pi_N$ ). This interpretation is supported by comparison with the spectra of parent phthalimide and its *N*-methyl derivative<sup>2,3</sup> and by OVGF calculations.

In the spectrum of **8** (Figure 1), signs of molecular ion fragmentation were observed. The appearance of a strong, sharp band at 10.87 eV suggests the presence of formaldehyde.<sup>10a</sup> Furthermore, the OVGF results for **8** differ from the measured spectrum, indicating that ion fragmentation took place. The observed spectrum (without the sharp 10.87 eV peak) is identical to the spectrum of phthalimide.<sup>2</sup> The photoinduced reaction of the aminium radical in the basic solution is known<sup>1</sup> and leads to elimination of formaldehyde via a retro-aldol fragmentation mechanism.<sup>1</sup>

Figure 4. HeI and HeII photoelectron spectra of **11** and **12**.

However, the fragmentation mechanism of **8** in vacuo can be described as a McLafferty-type rearrangement of radical cation which is well-known in mass spectrometry (Scheme 3). The mechanism involves hydrogen transfer from the OH to the CO group within the pseudo six-membered cyclic transition state followed by or concomitant with the elimination of formaldehyde. However, this is the first time that the fragmentation was detected in vacuo following the photoionization process (UPS).

The spectrum of **9** (Figure 2) shows a broad, poorly resolved cluster of bands with maxima at 9.25, 9.85, 10.15, and 10.4 eV. To interpret this spectrum, we used OVGF results. We also compared the spectrum of **9** with the spectra of **13**, *N*-(4-bromobutyl) and *N*-butylphthalimides,<sup>6</sup> phthalimide,<sup>2</sup> and methylhydroxylamines.<sup>11</sup> Taking all the results into account, we conclude that bands at 10.15 and 10.4 eV correspond to bromine lone pair ionizations, while the remaining bands in the cluster are attributed to orbitals similar to the parent phthalimide (Table 1). The oxygen lone pair of hydroxylamine moiety interacts (mixes) with the nitrogen lone pair which gives two orbitals best described as in-phase and out-of-phase linear combinations [ $n_{\text{NO}} \pm \pi_N$ ]. The sizable interaction between the phthalimide nitrogen lone pair and orbitals localized on substituents has been observed previously in, for example, *N*-vinylphthalimide.<sup>5</sup>

The spectrum of **10** (Figure 3) is consistent with the ionization energies calculated by the OVGF method (Table 1). We paid

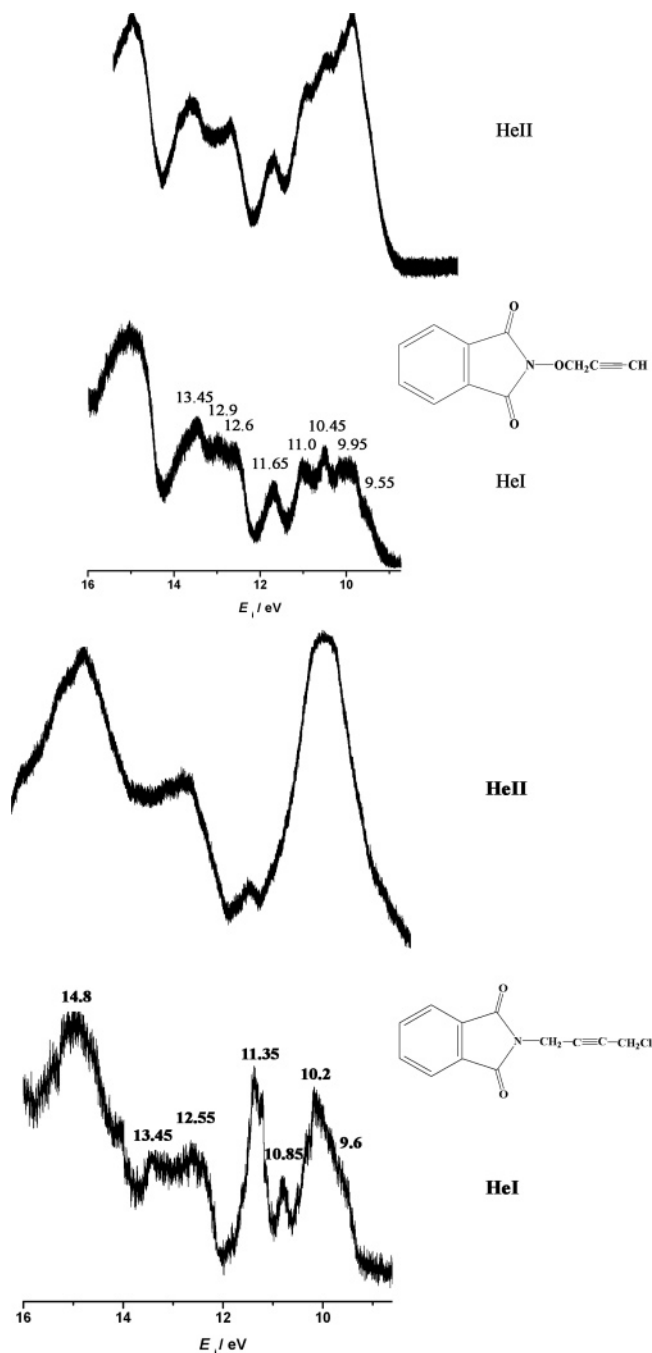
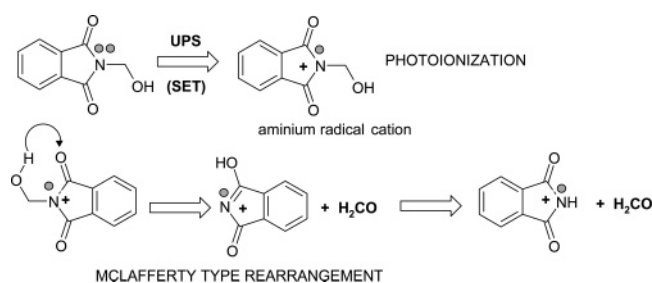


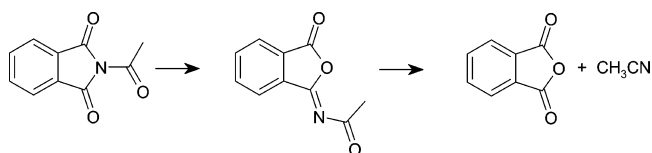
Figure 5. HeI and HeII photoelectron spectra of **13** and **14**.

### SCHEME 3



special attention to the possibility that there was phthalic anhydride present in the original sample, because phthalic anhydride is often used as the starting material in the preparation of **10**. The sample was therefore recrystallized, and its identity was checked by NMR, which confirmed it to be pure **10**. We

### SCHEME 4



started by comparing the ionization energies with the spectra of plausible deacetylation products (e.g., acetaldehyde, vinyl alcohol, and ketene). The reported photoelectron spectrum of ketene<sup>12</sup> exhibits a single band in the 9–14 eV region which has the ionization energy of 9.6 eV. This suggests that ketene ( $\text{H}_2\text{CCO}$ ) is not the likely fragmentation product. The isomers of ketene:ethanol ( $\text{H}_2\text{C}=\text{CHOH}$ )<sup>13</sup> and acetaldehyde<sup>14</sup> have been also studied by photoelectron spectroscopy. The unstable ethenol molecule shows bands at 9.17 and 9.30 eV and is thus also an unlikely fragmentation product. Acetaldehyde has a single, strong, and very sharp band at 10.26 eV that does not match the group of bands observed in the 10–12 eV region of **10**. This makes acetaldehyde also the unlikely fragmentation product. We also investigated the possibility that the recorded spectrum contains phthalic anhydride<sup>2</sup> as a photochemical degradation product (i.e., that it is a superposition of **10** with the phthalic anhydride as its major photochemical product; Scheme 4). The proposed photochemical reaction would involve N to O acyl migration as the intermediate step,<sup>1a</sup> which leads to the formation of iminolactone. The migration is similar to photo-Fries rearrangement and was previously observed in silylmethylimides.<sup>15</sup>

Subsequent fragmentation of iminolactone would lead to the elimination of acetonitrile<sup>15</sup> and the generation of phthalic anhydride according to Scheme 4. The spectrum of acetonitrile has the first broad band at 12.12 eV<sup>14</sup> which could be obscured by the numerous closely spaced bands of **10** and phthalic anhydride. However, there is no match between the spectrum in Figure 3 and phthalic anhydride, because the sharp band present at 11.30 eV in phthalic anhydride is not present in Figure 3. Furthermore, the comparison between spectra of **10** and **11** (Figures 3 and 4), which both have a keto group, further supports the conclusion that photodegradation of **10** into phthalic anhydride does not take place. This marked difference between the photochemical reactions in the gas phase and solution suggests that, for phthalimides, solvent molecules are the key factor that determines mechanisms and photochemical products.

The spectrum of **11** (Figure 4) shows two broad, unresolved manifolds with maxima at 10.0 and 11.25 eV. On the basis of relative manifold intensities as well as the OVG result, we conclude that the first manifold comprises five and the second two ionizations. The three carbonyl oxygen lone pairs are designated as  $n_{\text{O}}$  to emphasize their mixing (interaction), whereas the ester oxygen lone pair is designated as  $n_{\text{OEt}}$ . Comparison of **11** with the spectra of carbonyl derivatives, esters, and amides<sup>16,17</sup> suggests the assignment given in Table 1.

The spectrum of **12** (Figure 4) has broad, poorly resolved bands in the range 9.2–10.2 eV. The assignment, based on OVG results, is similar to the parent phthalimide except for the lowest energy band. In the photoelectron spectra of trimethylsilylamines, the decrease of the ionization energy of the nitrogen lone pair below 9 eV is well-established.<sup>18</sup> The decrease can be attributed to the very low effective nuclear charge on silicon (compared to carbon and especially to nitrogen) and subsequent polarization of the Si–N bond, which results in Si to N electron donation. The electron shift stabilizes



the radical cation reducing the ionization energy of  $\pi_N$ . The change in nitrogen lone pair ionization energy deduced from the spectrum of **12** is 1.36 eV. The remaining MO energies in **12** are affected by alkylsilyl substitution to a much smaller extent ( $\sim 0.3$  eV).

The spectrum of **13** (Figure 5) contains the cluster of partially resolved bands in the range 9.55–11.0 eV and a single band at 11.65 eV. The assignment is based on OVGf results, HeI/HeII intensity changes, and comparison with the spectra of methyl-ethyne,<sup>19</sup> phthalimide,<sup>2</sup> and methylhydroxylamines.<sup>11</sup> The relative intensity of bands at 9.55 and 9.95 eV is strongly enhanced at higher photon energy (HeII). We conclude that the corresponding MOs have oxygen and nitrogen lone pair character and correspond to ionizations from nitrogen lone pair ( $\pi_N$ ) and an out-of-phase linear combination of oxygen lone pairs ( $n_-$ ). The ionization from the orbital localized on ethyne moiety ( $\pi_{CC}$ ) can be attributed to 10.45 eV band by noting that in methyl-ethyne  $\pi_{CC}$  corresponds to the strong, sharp band at 10.37 eV. The narrow width of the 10.45 eV band further suggests ionization from a strongly localized orbital. The remaining bands can be attributed to ionizations from orbitals whose character is similar to the parent phthalimide (Table 1). The band at 11.65 eV can be attributed to ionization from the oxygen lone pair of the hydroxylamine moiety ( $n_{OR}$ ). This conclusion is supported by the OVGf result and by comparison with hydroxylamine where the oxygen lone pair appears at 11.74 eV.

The spectrum of **14** (Figure 5) contains band manifold at 9.6–10.2 eV, a single band at 10.85 eV, and two ionizations at 11.35 eV. The assignment is based on empirical arguments and OVGf results. Comparison with the spectrum of propargyl chloride,<sup>10b</sup> where  $\pi_{CC}$  ionizations are at 10.7–11.1 eV, suggests that in **14** the  $\pi_{CC}$  band appears at 10.85 eV. Chlorine lone pair ionizations can be readily attributed to the 11.35 eV band, because this band shows the strongest fall in intensity at higher photon energy. Also, in the related molecule propargyl chloride<sup>10b</sup> the chlorine lone pair ionizations appear at 11.7 eV. The unresolved 9.6–10.2 eV manifold comprises ionizations from the remaining five phthalimide orbitals:  $\pi_3$ ,  $n_-$ ,  $\pi_2$ ,  $\pi_N$ , and  $n_+$  as given in Table 1.

## Summary

We investigated the influence of N-substituents on the electronic structure and photochemistry of phthalimides. Photoelectron spectroscopy (due to its inferior resolution) is not the most suitable method for studying photochemical reactions. However, photochemical reactions observed by UPS take place in vacuo. UPS results can then be compared to analogous reactions taking place in solution, and thus further insight into SET reaction mechanisms can be gained. We have described photochemical reactions leading to fragmentation and elimination in the N-substituted phthalimides in vacuo and showed them to be different from the mechanisms prevailing in solution. The difference may be due to the presence of solvent molecules.

**Supporting Information Available:** Table showing the coordinates of optimized geometries, number of imaginary frequencies, and total energies. This material is available free of charge via the Internet at <http://pubs.acs.org>.

## References and Notes

- (1) (a) Yoon, U. C.; Mariano, P. S. *Acc. Chem. Res.* **2001**, *34*, 523. (b) Oelgemoller, M.; Griesbeck, A. G. *J. Photochem. Photobiol., C* **2002**, *3*, 109. (c) Antonello, S.; Maramba, F. *Chem. Soc. Rev.* **2005**, *34*, 418. (d) Yoon, U. C.; Su, Z.; Mariano, P. S. In *CRC Handbook of Organic Photochemistry and Photobiology*, 2nd ed.; Horspool, W. H., Lenci, F., Eds.; CRC Press: Boca Raton, FL, 2004; p 101.
- (2) (a) Galasso, V.; Colonna, F. P.; Distefano, G. *J. Electron Spectrosc. Relat. Phenom.* **1977**, *10*, 227. (b) Klasinc, L.; Trinajstić, N.; Knop, J. V. *Int. J. Quantum Chem., Quantum Biol. Symp.* **1980**, *7*, 403.
- (3) Distefano, G.; Jones, D.; Colonna, F. P.; Bigotto, A.; Galasso, V.; Pappalardo, G. C.; Scarlata, G. *J. Chem. Soc., Perkin Trans. 2* **1978**, 441.
- (4) Ajo, D.; Casarin, M.; Granozzi, G.; Croatto, U.; Bettoli, M. G. *J. Crystallogr. Spectrosc. Res.* **1984**, *14*, 349.
- (5) Ajo, D.; Casarin, M.; Granozzi, G.; Poli, A. *J. Crystallogr. Spectrosc. Res.* **1982**, *12*, 489.
- (6) Asfandiarov, N. L.; Prokopenko, I. A.; Bondarev, M. L. *J. Electron Spectrosc. Relat. Phenom.* **1992**, *58*, 177.
- (7) Yeh, J. J. *Atomic Calculation of Photoionization Cross-sections and Asymmetry Parameters*; Gordon and Breach: Langhorne, 1993.
- (8) Frisch, M. J.; Trucks, G. W.; Schlegel, H. B.; Scuseria, G. E.; Robb, M. A.; Cheeseman, J. R.; Zakrzewski, V. G.; Montgomery, J. A., Jr.; Stratmann, R. E.; Burant, J. C.; Dapprich, S.; Millam, J. M.; Daniels, A. D.; Kudin, K. N.; Strain, M. C.; Farkas, O.; Tomasi, J.; Barone, V.; Cossi, M.; Cammi, R.; Mennucci, B.; Pomelli, C.; Adamo, C.; Clifford, S.; Ochterski, J.; Petersson, G. A.; Ayala, P. Y.; Cui, Q.; Morokuma, K.; Malick, D. K.; Rabuck, A. D.; Raghavachari, K.; Foresman, J. B.; Cioslowski, J.; Ortiz, J. V.; Stefanov, B. B.; Liu, G.; Liashenko, A.; Piskorz, P.; Komaromi, I.; Gomperts, R.; Martin, R. L.; Fox, D. J.; Keith, T.; Al-Laham, M. A.; Peng, C. Y.; Nanayakkara, A.; Gonzalez, C.; Challacombe, M.; Gill, P. M. W.; Johnson, B.; Chen, W.; Wong, M. W.; Andres, J. L.; Gonzalez, C.; Head-Gordon, M.; Replogle, E. S.; Pople, J. A. *Gaussian 03*, revision B5; Gaussian, Inc.: Pittsburgh, PA, 2003.
- (9) Cederbaum, L. S.; Domcke, W. *Adv. Chem. Phys.* **1977**, *36*, 205.
- (10) (a) von Niessen, W.; Bieri, G.; Åsbrink, L. *J. Electron Spectrosc. Relat. Phenom.* **1980**, *21*, 175. (b) Bieri, G.; Åsbrink, L.; von Niessen, W. *J. Electron Spectrosc. Relat. Phenom.* **1982**, *27*, 129.
- (11) Rademacher, P.; Freckmann, B. *J. Electron Spectrosc. Relat. Phenom.* **1980**, *19*, 251.
- (12) Niu, B.-H.; Bai, Y.; Shirley, D. A. *Chem. Phys. Lett.* **1992**, *201*, 217.
- (13) Matti, G. Y.; Osman, I. O.; Upham, J. E.; Suffolk, R. J.; Kroto, H. W. *J. Electron Spectrosc. Relat. Phenom.* **1989**, *49*, 195.
- (14) Kimura, K.; Katsumata, S.; Achiba, Y.; Yamazaki, T.; Iwata, S. *Handbook of HeI Photoelectron Spectra of Fundamental Organic Molecules*; Japan Scientific Societies Press: Tokyo, 1981.
- (15) (a) Yoon, U. C.; Cho, S. J.; Lee, Y.-J.; Mancheno, M. J.; Mariano, P. S. *J. Org. Chem.* **1995**, *60*, 2353. (b) Iyer, P. S. Ph.D. Thesis, Duquesne University, 2003; p 42.
- (16) Jones, D.; Modelli, A.; Olivato, P. R.; Dal Colle, M.; de Paolo, M.; Distefano, G. *J. Chem. Soc., Perkin Trans. 2* **1994**, 1651.
- (17) Cannington, P. H.; Ham, N. S. *J. Electron Spectrosc. Relat. Phenom.* **1985**, *36*, 203.
- (18) Bock, H.; Solouki, B. In *The Chemistry of Organic Silicon Compounds*; Patai, S., Rappoport, Z. S., Eds.; Wiley: Chichester, 1989; Chapter 9, p 555.
- (19) Bieri, G.; Burger, F.; Heilbronner, E.; Maier, J. P. *Helv. Chim. Acta* **1977**, *60*, 2213.